PHYSICAL REVIEW B VOLUME 38, NUMBER 10 1 OCTOBER 1988

# Lower critical field of an anisotropic extreme type-II superconductor

Richard A. Klemm*
*Department of Physics B-019, University of California, San Diego, La Jolla, California 92093*
(Received 23 May 1988)

It is shown that the procedure of Klemm and Clem (abbreviated as I) for the transformation to isotropic form of the Ginzburg-Landau free energy for a superconductor with a general effective-mass anisotropy leads to a current which is *not* perpendicular to the magnetic induction **B**, unless **B** is in a crystal-symmetry direction. In general, the mean-field free energy is thus a function of a new parameter $\beta$, which depends upon the direction cosines of **B**, as well as a function of the renormalized $\tilde{\kappa}$ parameter of I, except at the upper critical field $H_{c2}$. A perturbation solution in $\gamma=\beta/(1+\beta)$ is found to order $\gamma^2$, and the angular dependence of the lower critical field $H_{c1}$ is determined. The parameter $\beta$ is found to cause **B** to nearly lock on to a crystal-symmetry direction, so that as the external field angle is varied, **B** switches from near to one symmetry direction to (near to) another, yielding a kink in the angular dependence of $H_{c1}$ that is more pronounced than in I.

## I. INTRODUCTION

Recently, an enormous amount of work has been performed on the superconducting properties of the new (high-$T_c$) materials with transition temperatures $T_c$ exceeding that of liquid nitrogen.[1-3] It has been found that the new materials are layered superconductors with anisotropies competitive with the intercalated dichalcogenides[4] such as $TaS_2$ (pyridine)$_{1/2}$. These new materials, $YBa_2Cu_3O_{7-\delta}$ and related compounds, have now been made of sufficient quality[5] that precise measurements of the anisotropies of the critical-field values are possible. In particular, Worthington and co-workers[5] showed that a single crystal of $YBa_2Cu_3O_{7-\delta}$ had an angular dependence of the upper critical field $H_{c2}$ near to $T_c$ that agreed precisely with the form expected for effective-mass anisotropy. Although such a form could also arise from order-parameter anisotropy,[6] it is well established that the normal-state properties are highly anisotropic, the carrier transport taking place predominantly within the layers, as in $TaS_2$ (pyridine)$_{1/2}$.[4] Since the pairing interaction is expected to be strongest within the layers as well, if the order parameter were to exhibit a nodal structure, it is most likely that such nodes would arise for quasiparticle motion normal to the layers. If such were the case, this would yield an $H_{c2}$ anisotropy that would be opposite to that observed. It is hence reasonable to expect that the dominant contribution to the $H_{c2}$ anisotropy arises from effective-mass anisotropy, although the actual effective-mass ratio might be larger than what one would infer from the measured $H_{c2}$ anisotropy.

In addition, recent measurements of the lower critical-field anisotropy on the high-$T_c$ materials have been made.[7,8] Although the earliest work on these materials did not appear to have been made on crystals with present-day perfection, and difficulty in determining $H_{c1}$ from the magnetization curves (presumably due to flux pinning) has complicated the interpretation of the results, it is inevitable that reliable results will be forthcoming.

The above mentioned recent excitement over high-$T_c$ materials has caused me to reexamine our previous work (I),[9] in the hope of gaining some new insights into the superconducting properties of these materials. In that work, we showed that the Ginzburg-Landau (GL) free energy for an anisotropic superconductor could be transformed to isotropic form, resulting in an effective GL parameter $\tilde{\kappa}$, which depends upon the direction cosines of the magnetic induction **B**. Although I believed our transformation procedure to be correct, I was disturbed by the subsequent results of Kogan and co-workers[10] which showed that in the London limit ($\tilde{\kappa}\rightarrow\infty$), there was a contribution to the current parallel to the local magnetic induction **B**, which we had not found. In addition, our results were in disagreement with the results of Tilley[11] for small anisotropies that the vortex structure just below $H_{c2}$ tended to lock onto the crystal lattice.

As I will demonstrate below, the resolution of these apparent paradoxes arises from the minimization of the transformed free energy. If one first minimizes the free energy and applies the Klemm-Clem transformation to the resulting (GL) mean-field equations, one finds a current parallel to **B**. The GL equations for the order parameter and for the two components of the vector potential (i.e., the current) normal to **B** are independent of the order of minimization. The correct procedure for the mean-field theory is to perform the minimization with respect to the bare (or gauge transformed) vector potential.

The component of the current parallel to **B** in the transformed variables is characterized by a single anisotropy parameter $\beta$, which vanishes at all crystal-symmetry directions. For a material with uniaxial symmetry, $\beta$ can be large for vortex directions away from the crystal axes. However, a perturbation expansion in $\gamma=\beta/(1+\beta)$ is found to be possible; such an expansion is performed to order $\gamma^2$. To each order in $\gamma$, the radial variation of the order parameter and the local magnetic induction pick up logarithmic terms which do not combine in any readily apparent way to give a single (or even angularly dependent) power law behavior for small radii. This perturbation treatment is then employed to estimate the variation of the order parameter in the intermediate regime (away from, but not too far from the vortex core), and used to calculate the vortex line energy to order $\gamma^2(\ln\tilde{\kappa})^2$. Nonvanishing $\gamma$ appears to always cost energy. The angular dependence of $H_{c1}$ is then found both for infinite samples and for general ellipsoids. It is found that for $\tilde{\kappa}$ values and effective-mass anisotropies expected for the high-$T_c$ materials, the vortex cores are always very close to a crystal-symmetry direction resulting in a discontinuity in the derivative of the angular dependence of $H_{c1}$. This kink is more pronounced than that predicted in I.

## II. TRANSFORMATION OF THE MEAN-FIELD EQUATIONS

In I, we investigated the fully anisotropic Ginzburg-Landau Helmholtz free energy, which in the reduced units after the usual gauge-transformation can be written in the form [Eq. (8) of I]

$$F_s-F_N=\int d^3r\left[-f^2+\tfrac{1}{2}f^4+\sum_\mu\frac{m}{m_\mu}\left[\frac{1}{\kappa^2}(\partial_\mu f)^2+a_\mu^2f^2\right]+b^2\right], \tag{1}$$

where $m=(m_1m_2m_3)^{1/3}$ is the effective-mass geometric mean, $\kappa=\lambda/\xi$ is the usual GL parameter, $\mathbf{b}=\nabla\times\mathbf{a}$ is the local magnetic induction in terms of the gauge-transformed [Eq. (7) of I] vector potential, $f=|\Psi/\Psi_0|$ is the relative magnitude of the local order parameter, $m_\mu$ is the effective mass in the $\mu=1$, 2, or 3 direction, and $\partial_\mu\equiv\partial/\partial x_\mu$. Note that Eq. (1) differs slightly in notation from Eq. (8) of I, in that we have redefined $f_0$ and $a_{0\mu}$ to be $f$ and $a_\mu$, respectively. The direction of $\mathbf{b}$ was assumed constant in the sample, $\mathbf{b}(\mathbf{r})=b(\mathbf{r})(\sin\theta_0\cos\phi_0, \sin\theta_0\sin\phi_0, \cos\theta_0)$. In I, we found that Eq. (1) could be transformed to isotropic form by an anisotropic scale transformation, a rotation, and an isotropic scale transformation, preserving Maxwell's equations in each step. These transformations together could be written as [Eq. (38) in I]

$$x_\mu=\frac{1}{\alpha}\left[\frac{m}{m_\mu}\right]^{1/2}\sum_v\lambda_{v\mu}\tilde{x}_v\,, \tag{2a}$$

$$\partial_\mu=\alpha\left[\frac{m_\mu}{m}\right]^{1/2}\sum_v\lambda_{v\mu}\tilde{\partial}_v\,, \tag{2b}$$

$$b_\mu=\alpha\left[\frac{m}{m_\mu}\right]^{1/2}\sum_v\lambda_{v\mu}\tilde{b}_v\,, \tag{2c}$$

and

$$a_\mu=\left[\frac{m_\mu}{m}\right]^{1/2}\sum_v\lambda_{v\mu}\tilde{a}_v\,, \tag{2d}$$

where

$$\alpha=\left[\sum_\mu\frac{m_\mu}{m}(\hat{\mathbf{e}}_\mu\cdot\hat{\mathbf{b}})^2\right]^{1/2} \tag{3}$$

is the anisotropy parameter relevant to the upper critical field $H_{c2}$. The unit vectors $\hat{\mathbf{e}}_\mu\equiv\hat{\mathbf{x}}_\mu$, and the rotation matrix $\lambda_{v\mu}$ is given by [Eq. (36) of I]

$$\lambda_{v\mu}=\begin{bmatrix}\sin\phi' & -\cos\phi' & 0\\ \cos\theta'\cos\phi' & \cos\theta'\sin\phi' & -\sin\theta'\\ \sin\theta'\cos\phi' & \sin\theta'\sin\phi' & \cos\theta'\end{bmatrix}. \tag{4}$$

The angles $\theta',\phi'$ are related to the direction cosines of $\mathbf{b}$ by

$$\sin\theta'\cos\phi'=\frac{1}{\alpha}\left[\frac{m_1}{m}\right]^{1/2}\sin\theta_0\cos\phi_0\,, \tag{5a}$$

$$\sin\theta'\sin\phi'=\frac{1}{\alpha}\left[\frac{m_2}{m}\right]^{1/2}\sin\theta_0\sin\phi_0\,, \tag{5b}$$

$$\cos\theta'=\frac{1}{\alpha}\left[\frac{m_3}{m}\right]^{1/2}\cos\theta_0\,, \tag{5c}$$

so that this unitary transformation rotates the axis (after the anisotropic scale transformation) so that the rotated $\hat{\mathbf{z}}$ axis lies parallel to the scale transformed $\mathbf{b}$. Hence, $\tilde{b}_v=\tilde{b}_3\delta_{v3}$. It should be noted, however, that using Eq. (2c) to write $b_\mu$ in terms of $\tilde{b}_v$ does not automatically set $\tilde{b}_1=\tilde{b}_2=0$, that must be done by using the inverse transformation to write $\tilde{b}_v$ in terms of $b_\mu$, and setting $\tilde{b}_1=\tilde{b}_2=0$. Rather than transform Eq. (1) using Eq. (2), we first minimize the free energy with respect to the untransformed variables, yielding

$$\sum_\mu\frac{m}{m_\mu}\left[-\frac{1}{\kappa^2}\partial_\mu^2f+a_\mu^2f\right]=f(1-f^2)\,, \tag{6a}$$

and

$$-\frac{m}{m_\mu}a_\mu f^2=[\nabla\times(\nabla\times\mathbf{a})]\cdot\hat{\mathbf{e}}_\mu=\sum_v\partial_v(\partial_\mu a_v-\partial_v a_\mu)\,. \tag{6b}$$

We now apply the transformations [Eq. (2)] to Eq. (6). It is easy to see that Eq. (6a) can be fully transformed as in I, yielding

$$-\frac{1}{\tilde{\kappa}^2}\tilde{\nabla}^2f+\tilde{a}^2f=f(1-f^2)\,, \tag{7}$$

where $\tilde{\kappa}=\kappa/\alpha$. Transformation of Eq. (6b) yields

$$-\sum_v\lambda_{v\mu}\tilde{a}_vf^2=\alpha^2\sum_{v,v',\lambda,\lambda'}\left[\frac{m_\mu m_v}{m^2}\right]\times\lambda_{\lambda v}(\lambda_{\lambda'\mu}\lambda_{v'v}-\lambda_{\lambda'v}\lambda_{v'\mu})\tilde{\partial}_\lambda\tilde{\partial}_{\lambda'}\tilde{a}_{v'}\,. \tag{8}$$

Multiplying by $\lambda_{\gamma\mu}$ and summing over $\mu$ gives

$$-\tilde{a}_\gamma f^2=\alpha^2\sum_{v',\lambda,\lambda'}(\Gamma_{\gamma\lambda'}\Gamma_{\lambda v'}-\Gamma_{\gamma v'}\Gamma_{\lambda\lambda'})\tilde{\partial}_\lambda\tilde{\partial}_{\lambda'}\tilde{a}_{v'}\,, \tag{9}$$

where

$$\Gamma_{\alpha\beta}\equiv\sum_v\frac{m_v}{m}\lambda_{\alpha v}\lambda_{\beta v}=\Gamma_{\beta\alpha}\,. \tag{10}$$

Explicit evaluation of Eq. (9) yields

$$\tilde{a}_1 f^2=-\tilde{\partial}_2\tilde{b}_3\,, \tag{11a}$$

$$\tilde{a}_2 f^2=\tilde{\partial}_1\tilde{b}_3\,, \tag{11b}$$

and

$$\tilde{a}_3 f^2=\epsilon_1\tilde{\partial}_1\tilde{b}_3+\epsilon_2\tilde{\partial}_2\tilde{b}_3\,, \tag{11c}$$

where

$$\epsilon_1\equiv\gamma^2(\Gamma_{32}\Gamma_{11}-\Gamma_{31}\Gamma_{12})=\frac{(m_3/m)^{1/2}\sin\theta_0\cos\theta_0\{(m/m_3)[(m_1/m)\cos^2\phi_0+(m_2/m)\sin^2\phi_0]-1\}}{[(m_1/m)\cos^2\phi_0+(m_2/m)\sin^2\phi_0]^{1/2}} \tag{12a}$$

and

$$\epsilon_2\equiv\gamma^2(\Gamma_{32}\Gamma_{21}-\Gamma_{31}\Gamma_{22})=\frac{(m_3/m)^{1/2}[(m_2-m_1)/m]\alpha\sin\theta_0\sin\phi_0\cos\phi_0}{[(m_1/m)\cos^2\phi_0+(m_2/m)\sin^2\phi_0]^{1/2}}\,. \tag{12b}$$

In deriving Eq. (11), use was made of the relations $\tilde{b}_1=\tilde{b}_2=0$, and the Maxwell equation $\tilde{\nabla}\cdot\tilde{\mathbf{b}}=0$. I remark that Eqs. (11a), (11b), and (7) are identical to those found in I by first transforming the free energy, and then minimizing with respect to the transformed variables. Equation (11c), however, could only be obtained by a transformation of the mean-field equations, and yields a component of the transformed vector potential (and hence the current) *parallel* to $\tilde{b}=\tilde{b}_3$. Apparently, the transformation procedure of I fixes the gauge, so that we are not free to choose $\tilde{a}_3=0$. Note that $\epsilon_1$ and $\epsilon_2$ both vanish for $\mathbf{b}$ in a crystal axis direction ($\mathbf{b}$ in the $\hat{\mathbf{x}}$, $\hat{\mathbf{y}}$, or $\hat{\mathbf{z}}$ directions); for an isotropic material they vanish identically. Although it appears at this point that two parameters (e.g., $\epsilon_1$ and $\epsilon_2$) characterize the parallel current, we shall see that only one combination of these parameters enters into the calculation.

Combining Eq. (11) with Eq. (7), we have

$$-\frac{1}{\tilde{\kappa}^2}\tilde{\nabla}^2 f+\frac{1}{f^3}[(\tilde{\partial}_2\tilde{b})^2+(\tilde{\partial}_1\tilde{b})^2+(\epsilon_1\tilde{\partial}_1\tilde{b}+\epsilon_2\tilde{\partial}_2\tilde{b})^2]=f(1-f^2)\,. \tag{13}$$

We also have $\tilde{b}=\tilde{\partial}_1\tilde{a}_2-\tilde{\partial}_2\tilde{a}_1$, which yields

$$\tilde{b}=\tilde{\partial}_1\left[\frac{1}{f^2}\tilde{\partial}_1\tilde{b}\right]+\tilde{\partial}_2\left[\frac{1}{f^2}\tilde{\partial}_2\tilde{b}\right]. \tag{14}$$

Equation (13) may be simplified by a rotation about the $\hat{\tilde{\mathbf{e}}}_3$ axis and by a change to cylindrical coordinates. Since $\tilde{\partial}_3\tilde{b}=0$, it is easily seen that a consistent solution of the above equations has $\tilde{\partial}_3 f=0$, so that the vortex cores do not vary spatially along their axes.

In cylindrical coordinates, Eq. (14) becomes

$$\tilde{b}=\frac{1}{\tilde{\rho}}\frac{\partial}{\partial\tilde{\rho}}\left[\frac{\tilde{\rho}}{f^2}\frac{\partial\tilde{b}}{\partial\tilde{\rho}}\right]+\frac{1}{\tilde{\rho}^2}\frac{\partial}{\partial\tilde{\phi}}\left[\frac{1}{f^2}\frac{\partial\tilde{b}}{\partial\tilde{\phi}}\right], \tag{15}$$

and Eq. (13) becomes

$$-\frac{1}{\tilde{\kappa}^2}\left[\frac{1}{\tilde{\rho}}\frac{\partial}{\partial\tilde{\rho}}\left[\tilde{\rho}\frac{\partial f}{\partial\tilde{\rho}}\right]+\frac{1}{\tilde{\rho}^2}\frac{\partial^2 f}{\partial\tilde{\phi}^2}\right]+\frac{1}{f^3}\left[\left(\frac{\partial\tilde{b}}{\partial\tilde{\rho}}\right)^2[1+(\epsilon_1\cos\tilde{\phi}+\epsilon_2\sin\tilde{\phi})^2]+\frac{1}{\tilde{\rho}^2}\left(\frac{\partial\tilde{b}}{\partial\tilde{\phi}}\right)^2[1+(\epsilon_1\sin\tilde{\phi}-\epsilon_2\cos\tilde{\phi})^2]\right.$$
$$\left.-\frac{1}{\rho}\frac{\partial\tilde{b}}{\partial\tilde{\rho}}\frac{\partial\tilde{b}}{\partial\tilde{\phi}}[(\epsilon_1^2-\epsilon_2^2)\sin2\tilde{\phi}-2\epsilon_1\epsilon_2\cos2\tilde{\phi}]\right]=f(1-f^2)\,. \tag{16}$$

Rotating about the $\tilde{z}$ axis by the angle $\phi_0$ given by

$$\tan2\phi_0=\frac{2\epsilon_1\epsilon_2}{\epsilon_1^2-\epsilon_2^2}\,, \tag{17}$$

one obtains

$$-\frac{1}{\tilde{\kappa}^2}\left[\frac{1}{\tilde{\rho}}\frac{\partial}{\partial\tilde{\rho}}\left[\tilde{\rho}\frac{\partial f}{\partial\tilde{\rho}}\right]+\frac{1}{\tilde{\rho}^2}\frac{\partial^2 f}{\partial\phi^2}\right]+\frac{1}{f^3}\left[\left(\frac{\partial\tilde{b}}{\partial\tilde{\rho}}\right)^2(1+\beta+\beta\cos2\phi)+\frac{1}{\tilde{\rho}^2}\left(\frac{\partial\tilde{b}}{\partial\phi}\right)^2(1+\beta-\beta\cos2\phi)\right.$$
$$\left.-\frac{2}{\tilde{\rho}}\frac{\partial\tilde{b}}{\partial\tilde{\rho}}\frac{\partial\tilde{b}}{\partial\phi}\beta\sin2\phi\right]=f(1-f^2)\,, \tag{18}$$

where

$$\beta = \tfrac{1}{2}(\epsilon_1^2 + \epsilon_2^2) \tag{19}$$

is the only combination of the parameters that enters the mean-field equations (and hence the minimized free energy), aside from the previously found parameter $\alpha$ that enters through $\tilde{\kappa}$. In Eq. (18), I have taken the liberty of redefining $\tilde{\phi} - \phi_0$ to be $\phi$, which also applies to Eq. (15).

Although it is possible to take Eqs. (15) and (18), together with the appropriate boundary conditions discussed below, as the starting point for the calculation of $f$, $b$, and the vortex line energy, we shall see that an exact solution of this problem for arbitrary $\beta$ is nontrivial. A perturbation solution for small $\beta$ is possible, however. Unfortunately, the parameter $\beta$ is not small for all angles and all effective-mass anisotropies. For a superconductor with uniaxial symmetry ($m_1 = m_2$), the parameter $\beta$ can be large both for filamentary ($m_1 > m_3$) and for layered ($m_3 > m_1$) symmetries, for $\theta_0 \simeq \pi/4$. Hence, it is useful to search for an effective expansion parameter that is more limited in its magnitude.

Examination of Eq. (18) reveals that the transformation

$$\tilde{\rho} = \rho\sqrt{1+\beta}\,, \tag{20}$$

together with the definition

$$\gamma \equiv \frac{\beta}{1+\beta}\,, \tag{21}$$

allow Eqs. (15) and (18) to be rewritten as

$$\frac{\tilde{b}}{1-\gamma} = \frac{1}{\rho}\frac{\partial}{\partial\rho}\left[\frac{\rho}{f^2}\frac{\partial\tilde{b}}{\partial\rho}\right] + \frac{1}{\rho^2}\frac{\partial}{\partial\phi}\left[\frac{1}{f^2}\frac{\partial\tilde{b}}{\partial\phi}\right] \tag{22}$$

and

$$-\frac{(1-\gamma)}{\tilde{\kappa}^2}\left[\frac{1}{\rho}\frac{\partial}{\partial\rho}\left[\rho\frac{\partial f}{\partial\rho}\right] + \frac{1}{\rho^2}\frac{\partial^2 f}{\partial\phi^2}\right] + \frac{1}{f^3}\left[\left[\frac{\partial\tilde{b}}{\partial\rho}\right]^2(1+\gamma\cos 2\phi) + \frac{1}{\rho^2}\left[\frac{\partial\tilde{b}}{\partial\phi}\right]^2(1-\gamma\cos 2\phi) - \frac{2}{\rho}\frac{\partial\tilde{b}}{\partial\phi}\frac{\partial\tilde{b}}{\partial\rho}\gamma\sin 2\phi\right] = f(1-f^2)\,. \tag{23}$$

Note that I have *not* transformed $\tilde{b}$, so that the relation $\tilde{\mathbf{b}} = \tilde{\nabla}\times\tilde{\mathbf{a}}$ is not preserved by this transformation. Hence, the boundary conditions are properly obtained in the $(\tilde{\rho},\phi)$ representation, and then scaled according to Eq. (20). It can be shown order by order in a perturbation expansion in $\beta$ that these different representations are identical. However, the advantage of $(\rho,\phi)$ representation is that the expansion parameter is $\gamma$, where $0 \le \gamma < 1$, so that the radius of convergence of the perturbation, if any, is greatly enhanced over that for the $\beta$ expansion, for systems with large anisotropy.

Equations (22) and (23) comprise the effective Ginzburg-Landau equations for a superconductor with a fully (diagonalized) effective-mass tensor. In order to solve them, one first needs to find the appropriate boundary conditions. We clearly require $f$ and $b$ to be continuous functions of $\rho$ and $\phi$. The explicit dependence of Eq. (23) upon $\phi$ is periodic, so we require

$$\tilde{b}(\rho,\phi) = \tilde{b}(\rho,\phi+2\pi)\,, \tag{24a}$$

$$f(\rho,\phi) = f(\rho,\phi+2\pi)\,. \tag{24b}$$

Since Eqs. (22) and (23) are symmetric under $\phi \to -\phi$, I choose solutions exhibiting that symmetry,

$$f(\rho,\phi) = f(\rho,-\phi)\,, \tag{25a}$$

$$\tilde{b}(\rho,\phi) = \tilde{b}(\rho,-\phi)\,. \tag{25b}$$

As $\rho \to \infty$, $f \to 1$ as for the $\gamma = 0$ case. As $\rho \to 0$, the appropriate boundary condition is obtained from the flux quantization,

$$\int_0^\infty d\rho\frac{\rho}{1-\gamma}\int_0^{2\pi} d\phi\,\tilde{b} = \frac{2\pi}{\tilde{\kappa}}\,. \tag{26}$$

Note that although the vector potential contains a component parallel to $\tilde{b}$, it is only the component $\tilde{a}_\phi$ which contributes to the closed line integral, just as in I. By using Eq. (22) in Eq. (26), the appropriate boundary condition as $\rho \to 0$ is found to be

$$\int_0^{2\pi} d\phi \frac{1}{2\pi}\frac{\rho(\partial\tilde{b}/\partial\rho)}{f^2}\bigg|_{\rho\to 0} = -\frac{1}{\tilde{\kappa}}\,. \tag{27}$$

Finally, one must calculate the line energy for a single vortex containing one flux quantum, which is the cost in energy per unit length of the vortex

$$\varepsilon(\tilde{\kappa},\gamma) = \frac{1}{(1-\gamma)}\int_0^{2\pi} d\phi\int_0^\infty d\rho\,\rho[\tilde{b}^2 + \tfrac{1}{2}(1-f^4)]\,. \tag{28}$$

Using the standard procedure[12] of multiplying Eq. (15) by $\partial\tilde{b}/\partial\tilde{\rho}$, Eq. (18) by $\partial f/\partial\tilde{\rho}$, and adding them together, I find after the transformation [Eq. (20)] that

$$\varepsilon(\tilde{\kappa},\gamma) = \varepsilon_{\rm reg} + \varepsilon_{\rm irreg}\,, \tag{29a}$$

where

$$\varepsilon_{\rm reg} = \frac{1}{(1-\gamma)}\int_0^{2\pi} d\phi\int_0^\infty d\rho\,\rho(1-f^2) \tag{29b}$$

and

$$\varepsilon_{\rm irreg} = -\int_0^{2\pi} d\phi\int_0^\infty d\rho\left[\frac{\partial\tilde{b}}{\partial\rho}\frac{\partial}{\partial\phi}\left[\frac{1}{f^2}\frac{\partial\tilde{b}}{\partial\phi}\right] - \frac{1}{\tilde{\kappa}^2}\frac{\partial f}{\partial\rho}\frac{\partial^2 f}{\partial\phi^2} + \frac{\gamma}{1-\gamma}(1+\cos 2\phi)\rho^2\frac{\partial f}{\partial\rho}\left[\frac{\partial\tilde{b}}{\partial\rho}\right]^2\Big/f^3 + \left[\frac{1+\gamma(1-\cos 2\phi)}{1-\gamma}\right]\frac{\partial f}{\partial\rho}\left[\frac{\partial\tilde{b}}{\partial\phi}\right]^2\Big/f^3 - \frac{2\gamma}{1-\gamma}\sin 2\phi\frac{\partial f}{\partial\rho}\frac{\partial\tilde{b}}{\partial\rho}\frac{\partial\tilde{b}}{\partial\phi}\Big/f^3\right]\,. \tag{29c}$$

Note that $\varepsilon_{\text{irreg}} \rightarrow 0$ as $\gamma \rightarrow 0$.

In order to calculate the line energy, it is necessary to consider two distinct regions of $\rho$. The dominant regime is for $\rho \gtrsim 1/\tilde{\kappa}$, which for $\gamma = 0$ gives the leading behavior for $\ln\tilde{\kappa} \gg 1$. However, we shall see that unlike the $\gamma = 0$ case, it is also necessary to investigate carefully the regime $0 \lesssim \rho \lesssim 1/\tilde{\kappa}$, which to order $\gamma$ gives a contribution to $\varepsilon$ of the same order in $\ln\tilde{\kappa}$. These corrections turn out to be numerically small, however.

## III. SOLUTION FOR SMALL $\gamma$

Although an exact solution of the problem for arbitrary $\gamma$ is not readily apparent, a perturbation expansion for small $\gamma$ can be readily obtained. We are interested primarily in the case $\ln\tilde{\kappa} \gg 1$, which is appropriate for the high-$T_c$ materials. In general, it will turn out that the effective "small" parameter is $\gamma \ln\tilde{\kappa}$.

I assume $b$ and $f$ may be expanded in powers of $\gamma$,

$$b = \sum_{n=0}^{\infty} b_n \gamma^n , \qquad (30a)$$

$$f = \sum_{n=0}^{\infty} f_n \gamma^n , \qquad (30b)$$

where $b_0$ and $f_0$ are independent of $\phi$ (as in the isotropic case). To evaluate the line energy in the dominant regime $1/\tilde{\kappa} \lesssim \rho$, it is first necessary to find the analytic form of the vortex core ($\rho \rightarrow 0$), as the boundary condition given by Eq. (27) can be used to approximate $f$ in the dominant regime.[12]

As for an isotropic superconductor with one flux quantum,[12] as $\rho \rightarrow 0$

$$f_0 = C_{00}\rho + O(\rho^3) , \qquad (31a)$$

$$b_0 = b_0(0) - a_{00}\rho^2 + O(\rho^4) , \qquad (31b)$$

where

$$a_{00} = \frac{C_{00}^2}{2\tilde{\kappa}} \qquad (32a)$$

and[13]

$$b_0(0) \cong \frac{1}{\tilde{\kappa}}(\ln\tilde{\kappa} - 0.289) . \qquad (32b)$$

The parameter $C_{00}$ has to be evaluated by a complete integration of the full solution.[13] I have investigated the terms of higher order in $\rho$ for an accurate calculation of the contribution to the line energy from the core region $0 \lesssim \rho \lesssim 1/\tilde{\kappa}$; such terms turn out to be unimportant both in the intermediate (dominant) regime and in the core region.

As $\rho \rightarrow 0$, a useful ansatz for $b_1$ and $f_1$ is

$$b_1 = a_{10}\rho^2 \ln\rho + a_{11}\rho^2 , \qquad (33a)$$

$$f_1 = C_{10}\rho \ln\rho + C_{11}\rho , \qquad (33b)$$

where $a_{ij}$ and $C_{ij}$ are functions of $\phi$. Let

$$\bar{a}_{ij} \equiv \frac{a_{ij}}{a_{00}} \qquad (34a)$$

and

$$\bar{C}_{ij} = \frac{C_{ij}}{C_{00}} . \qquad (34b)$$

Then Eq. (22) and the ansatz [Eq. (33)] yield as $\rho \rightarrow 0$,

$$\bar{a}_{10}'' = 0 \qquad (35a)$$

and

$$2\bar{a}_{10} + 4\bar{C}_{10} + \bar{a}_{11}'' = 0 . \qquad (35b)$$

Similarly, Eqs. (22) and (33) yield

$$4\bar{C}_{10} + \bar{C}_{10}'' + 2\bar{a}_{10} = 0 \qquad (36a)$$

and

$$4\bar{C}_{11} + \bar{C}_{11}'' + 2\bar{C}_{10} + \bar{a}_{10} + 2\bar{a}_{11} = 1 + \cos 2\phi . \qquad (36b)$$

Note that the terms in $\rho^2 \ln\rho$ and $\rho \ln\rho$ for $b_1$ and $f_1$ are necessary. If $\bar{a}_{10} = \bar{C}_{10} = 0$, for example, then $\bar{a}_{11}$ would have to be a constant from Eqs. (35b) and (24a), and then Eq. (36b) would have a secular term, causing $\bar{C}_{11}$ to lose its periodicity, in violation of Eq. (24b). Hence, the introduction of the terms proportional to $\ln\rho$ for $f_1/\rho$ and $b_1/\rho^2$ is required for the elimination of such secular terms.

It is easy to see that to order $\gamma$, the coefficients $\bar{C}_{1j}$ and $\bar{a}_{1j}$ satisfy

$$\bar{a}_{10} = \text{const} , \qquad (37a)$$

$$\bar{a}_{11} = \bar{a}_{110} + \tfrac{1}{4}\cos 2\phi , \qquad (37b)$$

$$\bar{C}_{10} = -\frac{\bar{a}_{10}}{2} + \tfrac{1}{4}\cos 2\phi , \qquad (37c)$$

$$\bar{C}_{11} = \tfrac{1}{4} - \tfrac{1}{2}\bar{a}_{110} + \bar{C}_{111}\cos 2\phi , \qquad (37d)$$

where $\bar{a}_{110}$ and $\bar{C}_{111}$ are constants of integration. We also have the boundary condition [Eq. (27)] which fixes $\bar{a}_{10}$,

$$\bar{a}_{10} = -1 . \qquad (38)$$

Equation (26) may be used to estimate $\bar{a}_{110}$ (of order unity, or, at most, $\ln\ln\tilde{\kappa}$), but an exact formula for it is not obvious, as a full calculation for arbitrary $\rho$ is required, just as in the calculation of $C_{00}$. The parameter, $\bar{C}_{111}$ appears to be arbitrary, and can be set equal to 0. Neither $\bar{a}_{110}$ nor $\bar{C}_{111}$ enter the leading corrections as $\rho \rightarrow 0$ of the higher-order solutions.

To second order in $\gamma$, the forms for $f_2$ and $b_2$ as $\rho \rightarrow 0$ required to eliminate the secular terms are

$$b_2 = a_{20}\rho^2(\ln\rho)^2 + a_{21}\rho^2\ln\rho + a_{22}\rho^2 , \qquad (39a)$$

$$f_2 = C_{20}\rho(\ln\rho)^2 + C_{21}\rho\ln\rho + C_{22}\rho . \qquad (39b)$$

By the procedure described above for the first-order solution, the coefficients in Eq. (39) are found to be

$$\bar{a}_{20} = -\tfrac{1}{4} , \tag{40a}$$

$$\bar{a}_{21} = \bar{a}_{110} + 2\bar{C}_{111} - \tfrac{7}{8} , \tag{40b}$$

$$\bar{a}_{22} = \bar{a}_{220} - (\bar{C}_{111} + \tfrac{1}{2}\bar{a}_{110} - \tfrac{3}{16})\cos 2\phi - \tfrac{1}{192}\cos 4\phi , \tag{40c}$$

$$\bar{C}_{20} = \tfrac{1}{64}(3 - \cos 4\phi) , \tag{40d}$$

$$\bar{C}_{21} = \tfrac{1}{4}(\tfrac{15}{8} - \bar{a}_{110} - \tfrac{5}{2}\bar{C}_{111}) + \tfrac{1}{4}(1 - 2\bar{C}_{111} - \tfrac{1}{2}\bar{a}_{110})\cos 2\phi - (\tfrac{1}{8}\bar{C}_{111} - \tfrac{1}{96})\cos 4\phi , \tag{40e}$$

$$\bar{C}_{22} = -\tfrac{1}{2}\bar{a}_{220} - \tfrac{1}{4}(\bar{a}_{110} + \bar{a}_{110}^2) - \tfrac{3}{4}(\bar{C}_{111} + 2\bar{C}_{111}^2) + \tfrac{27}{16} + \bar{C}_{221}\cos 2\phi + (\tfrac{1}{24}\bar{C}_{111} - \tfrac{1}{4}\bar{C}_{111}^2 + \tfrac{19}{1052})\cos 4\phi . \tag{40f}$$

Note that the two new constants of integration $\bar{a}_{220}$ and $\bar{C}_{221}$ are introduced. Note further that the earlier constants of integration $\bar{a}_{110}$ and $\bar{C}_{111}$ do not contribute to the leading behavior as $\rho \to 0$, given by the respective terms with the highest power of $\ln\rho$.

It is apparent that the $n$th-order solution is of the form

$$b_n(\phi) = \sum_{m,p=0}^{n} C_{nmp}\rho^2(\ln\rho)^{n-m}\cos(2p\phi) , \tag{41a}$$

$$f_n(\phi) = \sum_{m,p=0}^{n} a_{nmp}\rho(\ln\rho)^{n-m}\cos(2p\phi) , \tag{41b}$$

where the dominant coefficients $C_{nop}$ and $a_{nop}$ do not depend upon the various constants of integration.

We would like to find an expression for $f$ in the intermediate regime $1/\tilde{\kappa} \le \rho \ll \infty$. To do so, I employ Eq. (23), rewriting such terms as $(1/f^3)(\partial b/\partial\rho)^2$ as $(1/f^4)(\partial b/\partial\rho)^2 f$, and approximating $(1/f^4)(\partial b/\partial\rho)^2$ by $[(1/f^2)(\partial b/\partial\rho)|_{\rho\to 0}]^2$. Similarly, I approximate $(1/\rho f^2)(\partial b/\partial\phi)$ by its limiting behavior as $\rho \to 0$. This is a simple generalization of the standard asymptotic expansion[12-14] used for isotropic superconductors.

I find to $O(\gamma^2)$,

$$1 - f^2 \approx \frac{1}{\tilde{\kappa}^2\rho^2}\Big(1 + \gamma\cos 2\phi(\tfrac{1}{2} - \bar{C}_{111} - \tfrac{1}{4}\ln\rho) + \gamma^2\{(\ln\rho)^2(\tfrac{1}{8} + \tfrac{1}{2}\cos 2\phi + \tfrac{5}{16}\cos 4\phi) + \ln\rho(\bar{C}_{111} + \tfrac{17}{8}) + [\tfrac{33}{128} + \tfrac{9}{4}(\bar{a}_{110} - \bar{a}_{110}^2) - \tfrac{1}{2}\bar{C}_{111} - 3\bar{C}_{111}^2)]\} + O(\gamma^3)\Big) , \tag{42}$$

where terms proportional to $\cos 2\phi$ and $\cos 4\phi$ in the constant $\ln\rho$ coefficients of the $O(\gamma^2)$ term have been dropped, as they do not contribute to the line energy. The dominant contribution to the line energy is thus readily found to be

$$\varepsilon(\tilde{\kappa},\gamma) \approx \frac{2\pi}{(1-\gamma)\tilde{\kappa}^2}\left[\ln\tilde{\kappa} + 0.497 + \frac{\gamma^2(\ln\tilde{\kappa})^3}{24} + O[(\gamma^3)(\ln\tilde{\kappa})^4]\right] , \tag{43}$$

where I have neglected terms of order $\gamma^2(\ln\tilde{\kappa})^2$ in the brackets, assuming $\ln\tilde{\kappa} \gg 1$. The constant term in the brackets is included in order to closely approximate the correct answer as $\gamma \to 0$. Note that the apparent expansion parameter is $\gamma\ln\tilde{\kappa}$, and that it costs energy for the vortex to be directed off a crystal-symmetry direction ($\gamma \ne 0$). In the London limit $\tilde{\kappa} \to \infty$, the energy cost for a vortex to be off a crystal-symmetry direction is apparently divergent; the vortices lock onto the crystal lattice. For finite $\tilde{\kappa}$, however, they are constrained to be near to a crystal lattice direction, but do not lock onto it precisely. Note further that the prefactor $(1-\gamma)^{-1}$ is valid to all orders in $\gamma$, arising from the transformation of $\tilde{\rho}$ to $\rho$. Hence, as the effective-mass anisotropy becomes large (even if $\tilde{\kappa}$ is not too large), the vortices still greatly prefer to be near a crystal-symmetry direction.

Although in the isotropic limit, the contribution to the integral in $\varepsilon_{\text{reg}}$ from $0 \le \rho \lesssim 1/\tilde{\kappa}$ leads only to a term of order $\tilde{\kappa}^{-2}$ (and not $\tilde{\kappa}^{-2}\ln\tilde{\kappa}$), contributing[13] to the constant 0.497 in Eq. (43), for $\gamma \ne 0$ the $\ln\rho$ dependence of $f$ also gives a $\tilde{\kappa}^{-2}\ln\tilde{\kappa}$ contribution. I have evaluated the contribution to $\varepsilon_{\text{reg}}$ in this regime by the following scheme: expand $f_0$ and $b_0$ to order $\rho^3$ and $\rho^4$, respectively, and expand $f_1$ and $b_1$ to order $\rho^3\ln\rho$ and $\rho^4\ln\rho$, respectively. I have used the published results[13] for the above constant (0.497) to estimate $C_{00}$, and evaluated the integral. The result is a correction term

$$\varepsilon_{\text{reg corr}} \cong \frac{2\pi\gamma\ln\tilde{\kappa}(0.003)}{\tilde{\kappa}^2(1-\gamma)} , \tag{44}$$

which is negligible compared with Eq. (43) to order $\gamma$.

Finally, I have investigated the contribution from $\varepsilon_{\text{irreg}}$. To every order in $\gamma$ they contribute terms which are of at least one power in $\ln\tilde{\kappa}$ less than the corresponding terms in $\varepsilon_{\text{reg}}$. Hence, these terms can be neglected for $\ln\tilde{\kappa} \gg 1$. To a good approximation, the vortex line energy is given by Eq. (43).

## IV. ANGULAR DEPENDENCE OF $H_{c1}$

The calculation of the lower-critical field $H_{c1}$ is now elementary. The magnetic energy is

$$F_m = 2\mathbf{h}_e \cdot \mathbf{B} , \tag{45}$$

where $\mathbf{B}$ is the macroscopic magnetic induction and $\mathbf{h}_e$ is the external field. Since $B$ is given by the flux quantization condition [Eq. (26)],

$$B = \frac{2\pi}{\tilde{\kappa}} , \tag{46}$$

independent of $\gamma$. We therefore have for the component $\mathbf{h}_{c1}$ parallel to the local magnetic induction, $\mathbf{b}$,

$$H_{c1,\parallel} \cong \frac{1}{2\tilde{\kappa}(1-\gamma)}\left[\ln\tilde{\kappa}+0.497+\frac{\gamma^2(\ln\tilde{\kappa})^3}{24}\right]. \quad (47)$$

As in I, the full $\mathbf{h}_{c1}$ is found from

$$\mathbf{H}_{c1} = \hat{\mathbf{b}}H_{c1,\parallel} + \hat{\boldsymbol{\theta}}_0 \frac{\partial H_{c1,\parallel}}{\partial \theta_0} + \frac{\hat{\boldsymbol{\phi}}_0}{\sin\theta_0}\frac{\partial H_{c1,\parallel}}{\partial \phi_0}. \quad (48)$$

Note that both $\tilde{\kappa}$ and $\gamma$ depend upon the angles $\theta_0$ and $\phi_0$ describing the orientation of $\mathbf{b}$ in the original reference frame.

Since the materials of primary interest are layered in structure forming fairly flat rectangular prisms,[5] the demagnetization factors associated with the crystal shape must also be incorporated in order to compare with experiment. In an earlier paper,[15] I presented a treatment of the role of the demagnetization upon the lower critical field for a general ellipsoid. I will not elaborate upon that treatment, but will present some calculations for the case of uniaxial symmetry, assuming the effective-mass axes coincide with the ellipsoid (gross) crystal shape axes. Results both for layered and for filamentary symmetry will be presented.

## V. RESULTS AND DISCUSSION

In Fig. 1, I have plotted $H_{c1}$ as a function of $\theta_H$, the angle $\mathbf{H}$ makes with the $\hat{\mathbf{z}}$ axis for a material with layered symmetry ($m_1 = m_2$) with anisotropy parameter $\epsilon = m_1/m_3 = 0.1$, and $\kappa_< = 10$ and 50, where $\kappa_<$ is the minimum value of $\kappa$, which occurs for $\theta_H = 0$. Although in I no cusp in the angular dependence of $H_{c1}$ was predicted for $\epsilon$ values this large, cusps are clearly evident in these curves. The cusps occur at an angle $\theta_H^*$, at which the direction of $\mathbf{B}$ switches from near to one crystal-symmetry direction to near to another. In addition, I have plotted the function $\gamma(\theta_H)$ for these respective curves. Note that $\gamma(\theta_H) \neq 0$ except at the crystal-symmetry directions ($\theta_H = 0°$ and 90°), and exhibits a discontinuity at $\theta_H^*$. The nonvanishing $\gamma$ values tend to restrict $\mathbf{B}$ to point near to a crystal-symmetry direction, but this restriction is most pronounced near the hard direction ($\theta_0$ near to 0°). At $\theta_H^*$, $\theta_0$ jumps from $\sim$5.0° to 79.0° for $\kappa_< = 10$, and from $\sim$4.4° to 79.0° for $\kappa_< = 50$. Hence, increasing $\kappa_<$ tends to further favor the locking onto the harder crystal-symmetry direction. Note further that $\gamma$ never becomes very large, reaching a maximum in the neighborhood of 0.1 before the switching occurs, so the perturbation expansion in powers of $\gamma \ln\tilde{\kappa}$ (which is $\leq 0.33$) appears to be at least asymptotically valid, aided by the small coefficient of the $(\gamma \ln\tilde{\kappa})^2$ correction to the vortex line energy.

In Fig. 2, I have plotted the external field for first flux entry $H_E$ as a function of the external applied field angle $\theta_E$, for $\epsilon = 0.01$ and $\kappa_< = 50$. The solid curve corresponds to a bulk sample; $\theta_E = \theta_H$. The dashed curve is for an oblate spheroid with $c/a = 0.1$. Note that the cusplike behavior is not very different than in I (with $\gamma = 0$), as the anisotropy of $\tilde{\kappa}$ is responsible for most of the switching. The main difference from I is the upward curvature of $H_E(\theta_E)$ for small $\theta_E$. Note that demagnetization effects can remove the apparent anisotropy as well as the position of the cusp. At $\theta_E^*$, $\theta_0$ switches from 0.16° to 87.5°, independent of sample shape.

In Fig. 3, curves of $H_E(\theta_E)$ for $\kappa_< = 50$, $\epsilon = 0.001$ are shown for a bulk sample (solid curve) and an oblate spheroid with $c/a = 0.1$ (dashed curve). Again the behavior is almost quantitatively identical to that of I, differing primarily in the curvature of $H_E$ for small $\theta_E$. At $\theta_E^*$, $\theta_0$ switches from 0.01° to 89.3°, independent of sample shape.

Hence, the inclusion of the nonparallel currents does tend to cause the vortices to prefer to lie near a crystal-symmetry direction, but these currents have the largest effect on the measured $H_{c1}$ systems that are not very anisotropic. For highly anisotropic systems ($\epsilon \lll 1$), the Klemm-Clem formula ($\gamma = 0$) is pretty good.

In Fig. 4, I have attempted to fit the data of Denhoff

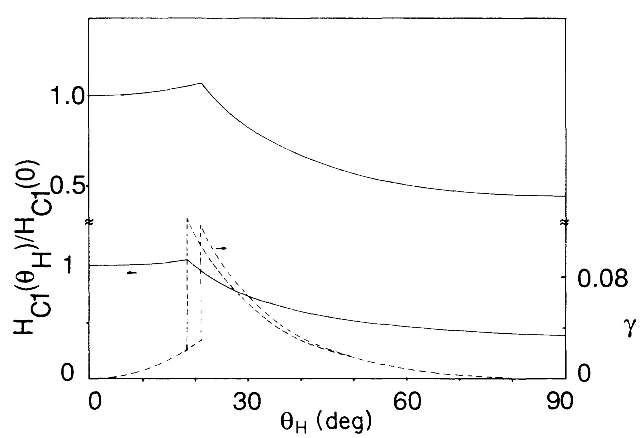


FIG. 1. The solid lines are plots of $H_{c1}(\theta_H)$ for a bulk sample with $\epsilon = 0.1$ for $\kappa_< = 10$ (upper) and $\kappa_< = 50$ (lower). The broken curves are plots of $\gamma(\theta_H)$ corresponding to the respective $H_{c1}$ curves.

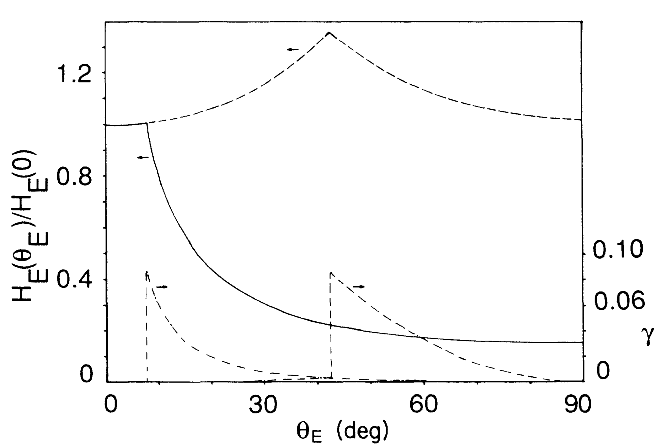


FIG. 2. Plots of the angular dependence of the applied field for first flux entry $H_E(\theta_E)$, normalized to its $\theta_E = 0$ value for $\epsilon = 0.01$ and $\kappa_< = 50$. Solid curve: bulk sample. Dashed curve: $c/a = 0.1$. The broken curves are the respective $\gamma$ values.

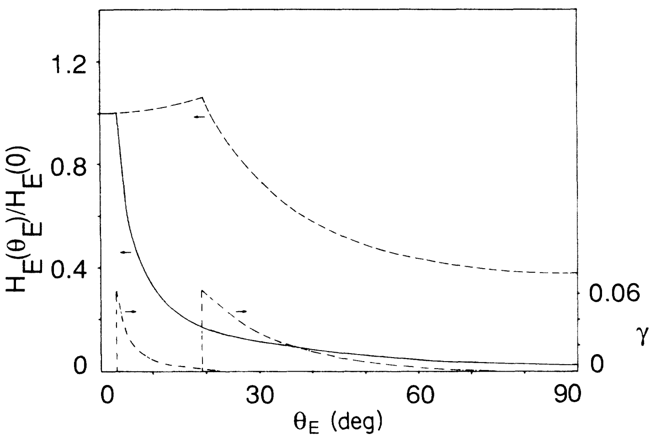


FIG. 3. Plots of $H_E(\theta_E)/H_E(0)$ for $\epsilon=0.001$ and $\kappa_<=50$. Solid curve: bulk sample. Dashed curve: $c/a=0.1$. The broken curves are the respective $\gamma$ values.

and Gygax[16] for the layered superconductor $NbSe_2$. Using their demagnetization parameters (corresponding to an oblate spheroid with $c/a=0.053$), the predicted applied field for the first flux entry $H_E$ as a function of the applied field angle $\theta_E$ is shown. The solid curve corresponds to $\epsilon=0.0375$, which is chosen to fit the data at $\theta_E=0°$ and 90°, respectively. The dashed curve is for $\epsilon=0.0625$, which was inferred from $H_{c2}$ measurements.[16] For $\theta_E \lesssim 70°$, the data fit on the predicted curve, but this was also true in their fit to the Klemm-Clem formula. However, unlike the earlier fit in which only the $\epsilon=0.0375$ predicted curve exhibited a cusp, both curves shown here exhibit cusps. In the region $70° < \theta_E \lesssim 90°$, the data fall between the two curves.

Although Denhoff and Gygax[16] were able to obtain a quantitative fit by assuming that **B** is only pointed in either of the two crystal axis directions, the present theory gives a partial justification for that assumption. These values of the parameters are not that different than in Fig. 1, so **B** is only constrained to lie near to one of the axes.

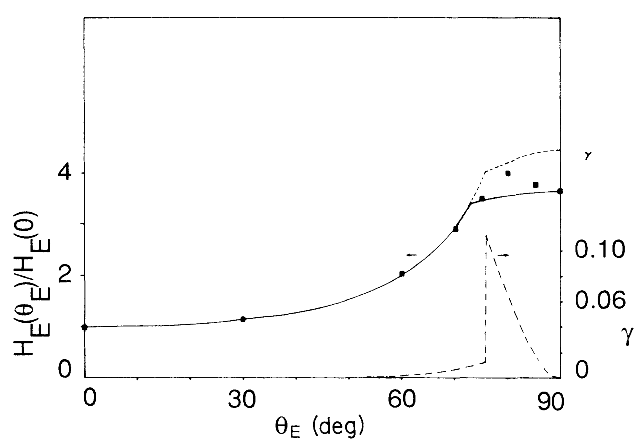


FIG. 4. Plot of $H_E(\theta_E)/H_E(0)$ for $\kappa_<=13.5$, $c/a=0.053$, $\epsilon=0.0625$ (dashed), and 0.0375 (solid). The broken curve is the $\gamma$ value corresponding to $\epsilon=0.0625$. The data are from Denhoff and Gygax (Ref. 16).

For the $\epsilon=0.0625$ curve, $\theta_0$ switches from 2.5° to 82.2°. For $\epsilon=0.0375$, $\theta_0$ switches from 1.2° to 84.5°. The variation of $\theta_0$ from 90° by the above amounts is reflected in the curvature of $H_E(\theta_E)$ near to $\theta_E=90°$, which is downward in the theoretical fit (although much less so than in the fit to the Klemm-Clem formula), whereas the experiment shows an upward curvature.

It should be noted that the anisotropy ($\epsilon=0.0625$) inferred from the $H_{c2}$ data would be modified if the order parameter exhibited some anisotropy. This could cause the inferred $\epsilon$ from $H_{c2}$ measurements to be larger than its intrinsic effective-mass value, which could possibly explain the low value of the observed $H_E(90°)$. An order-parameter anisotropy of $\sim 1.7$ can be inferred from a comparison of far-infrared[17] and tunneling[18] measurements. However, this theory does not take account of order-parameter anisotropy, so it is not known how that anisotropy might affect the angular dependence of $H_{c1}$ near the easy axis. Certainly, the layered structure of $NbSe_2$ would be expected to manifest itself most prominently for fields nearly parallel to the layers. The $H_{c2}$ behavior, however, tends to suggest that the vortex cores always extend over more than one layer, so naively one would expect this theory to be appropriate.

It should also be noted that $NbSe_2$ is rather anomalous in a number of its superconducting properties. For example, in Ref. 4, it was shown that the fluctuation diamagnetism of $NbSe_2$ just above $T_c$ did not fit the usual behavior for either a bulk or layered superconductor.

For completeness, I have also included some plots for superconductors with filamentary symmetry, $m_1=m_2>m_3$; $\epsilon \equiv m_3/m_1$. In Fig. 5, I have plotted $H_E(\theta_E)$, normalized to its $\theta_E=0$ value (parallel to the filament axis) for $\epsilon=10^{-1}$, $10^{-2}$, and $10^{-3}$ for bulk samples and for a prolate spheroid ($c/a=0.1$ for $\epsilon=0.1$, $c/a=0.01$ for $\epsilon=0.01$ and 0.001), and for $\kappa_<=10$. For $\epsilon=0.1$ and 0.001, I have also included curves for $\kappa_<=50$. The behavior is similar to that of the Klemm-Clem formula,[19]

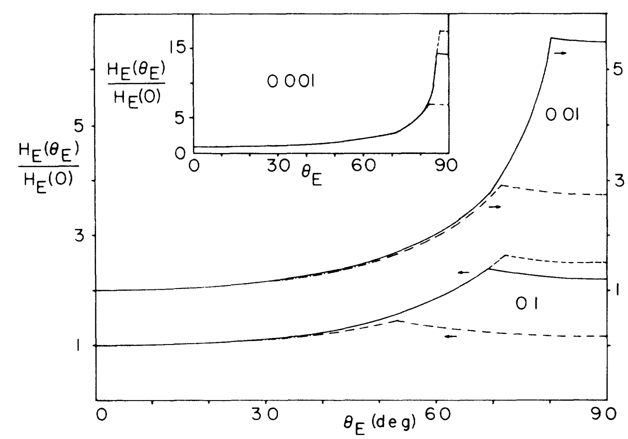


FIG. 5. Shown are plots of $H_E(\theta_E)/H_E(0)$ for filamentary superconductors with $\epsilon=0.1$, 0.01, and (inset) 0.001. Solid lines are for $\kappa_<=10$ for bulk ($c/a=1$) samples. Dashed curves are for bulk samples with $\kappa_<=50$. Dotted-dashed curves are for $\kappa_<=10$, and a sample of prolate spheroidal shape with $c/a=0.1$ for the $\epsilon=0.1$ curve, $c/a=0.01$ otherwise.

except for the curvature near to $\theta_E \sim 90°$, which has changed sign as for the curves with layered symmetry. Also, the $\epsilon = 0.1$ curves exhibit a cusp, which was not found previously.[20]

In conclusion, it has been shown that the transformation procedure of I leads to a component of the local current parallel to the local magnetic induction, even under the assumption that the direction of **b** is a constant in the sample. This parallel current tends to lock the vortices onto the crystal axes, but not rigidly, as **b** can point slightly away from the crystal axes, the amount dependent upon the anisotropy parameter $\epsilon$ and upon the vortex stiffness $\tilde{\kappa}$. In the London limit, this locking becomes rigid, as the asymptotic expansion in powers of $\gamma \ln \tilde{\kappa}$ breaks down as $\tilde{\kappa} \rightarrow \infty$. The near locking onto the crystal axis directions (found for a unidirectional vortex core) would most likely inhibit any entanglement of vortices which has been recently suggested.[21]

The question of the convergence of the perturbation series in $\gamma \ln \tilde{\kappa}$ remains open. The leading term found here is suggestive of convergence for $\gamma \ln \tilde{\kappa}$ not too large, so that the series appears to be at least asymptotically valid. Furthermore, the switching angles occur for rather small $\gamma \ln \tilde{\kappa}$, except for systems with small anisotropy. For a high degree of anisotropy ($\epsilon \lll 1$) one can essentially set $\gamma = 0$.

For a quantitative comparison with experiments on the high-$T_c$ materials, one ought to treat the demagnetization effects (for a real crystal with corners) in a better fashion than as an ellipsoid considered here. Also, the question of order-parameter anisotropy has not yet been satisfactorily resolved, as some experiments[22] are suggestive of a rather isotropic order parameter, whereas others[23] are suggestive of a nodal structure. It would also be desirable to perform the calculation for Josephson-coupled layers.[24] Such a calculation could be done below the dimensional crossover temperature for the field parallel to the layers, but does not appear at first sight to be easily solvable for **b** in an arbitrary direction. Such calculations are presently being performed, and will be discussed in subsequent publications.[25]

## ACKNOWLEDGMENTS

Ames Laboratory is operated for the U.S. Department of Energy by Iowa State University under Contract No. W-7405-ENG-82. This investigation was supported in part by the Director for Energy Research, Office of Basic Energy Sciences.

---

*Present address: Ames Laboratory, Department of Physics, Iowa State University, Ames, IA 50011.

[1] M. K. Wu *et al.*, Phys. Rev. Lett. **58**, 908 (1987); R. J. Cava *et al.*, *ibid.* **58**, 1676 (1987).

[2] A. Ourmazd, J. A. Rentschler, W. J. Skocpol, and D. W. Johnson, Jr., Phys. Rev. B **36**, 8914 (1987).

[3] P. L. Gammel, D. J. Bishop, G. J. Dolan, J. R. Kwo, C. A. Murray, L. F. Schneemeyer, and J. V. Waszczak, Phys. Rev. Lett. **59**, 2592 (1987).

[4] D. E. Prober, M. R. Beasley, and R. E. Schwall, Phys. Rev. B **15**, 5245 (1977); A. H. Thompson, Solid State Commun. **13**, 1911 (1973); R. A. Klemm, Ph.D. thesis, Harvard University, 1974 (unpublished).

[5] T. Worthington, Bull. Am. Phys. Soc. **33**, 685 (1988); T. K. Worthington, W. J. Gallagher, D. L. Kaiser, F. H. Holtzberg, and T. P. Dinger, Physica C **153–155**, 32 (1988); T. R. Dinger, T. K. Worthington, W J Gallagher, and R. L. Sandstrom, Phys. Rev. Lett. **58**, 2687 (1987).

[6] K. Scharnberg and R. A. Klemm, Phys. Rev. Lett. **54**, 2445 (1985).

[7] G. Crabtree, Bull. Am. Phys. Soc. **33**, 337 (1988).

[8] T. K. Worthington, W. J. Gallagher, and T. R. Dinger, Phys. Rev. Lett. **59**, 1160 (1987).

[9] R. A. Klemm and J. R. Clem, Phys. Rev. B **21**, 1868 (1980).

[10] V. G. Kogan, Phys. Rev. B **24**, 1572 (1981); V. G. Kogan and J. R. Clem, *ibid.* **24**, 2497 (1981).

[11] D. R. Tilley, Proc. Phys. Soc. London **85**, 1177 (1965).

[12] D. Saint-James, G. Sarma, and E. J. Thomas, *Type-II Superconductivity* (Pergamon, New York, 1969), pp. 46–51.

[13] C.-R. Hu, Phys. Rev. B **6**, 1756 (1972).

[14] A. A. Abrikosov, Zh. Eksp. Teor. Fiz. **32**, 1442 (1957) [Sov. Phys. JETP **5**, 1174 (1957)].

[15] R. A. Klemm, J. Low Temp. Phys. **39**, 589 (1980).

[16] M. W. Denhoff and S. Gygax, Phys. Rev. B **25**, 4479 (1982).

[17] B. P. Clayman and R. F. Frindt, Solid State Commun. **9**, 1881 (1971).

[18] R. C. Morris and R. V. Coleman, Phys. Lett. **43A**, 11 (1973).

[19] R. A. Klemm, in *Electronic Properties of Inorganic Quasi-One-Dimensional Materials, I,* edited by P. Monceau (Reidel, Boston, 1985), pp. 208–210.

[20] Note that the curves in Ref. 9 for filamentary superconductors resulted from a sign error in the numerical evaluation of the plots. The correct curves were presented in Ref. 19. This was pointed out to me by H. Schwenk.

[21] D. R. Nelson, Phys. Rev. Lett. **60**, 1973 (1988).

[22] D. R. Harshmann *et al.*, Phys. Rev. B **36**, 2386 (1987).

[23] J. R. Cooper *et al.*, Phys. Rev. B **37**, 638 (1988).

[24] W. Lawrence and S. Doniach, in *Proceedings of the Twelfth International Conference on Low Temperature Physics,* edited by Elizo Kanda (Academy of Japan, Kyoto, 1972), p. 361; R. A. Klemm, Ph.D. thesis, Harvard University, 1974 (unpublished).

[25] R. A. Klemm (unpublished).